AIP | Applied Physics Letters

Epitaxial growth of high mobility Bi2Se3 thin films on CdS

X. F. Kou, L. He, F. X. Xiu, M. R. Lang, Z. M. Liao et al.

Citation: Appl. Phys. Lett. **98**, 242102 (2011); doi: 10.1063/1.3599540
View online: http://dx.doi.org/10.1063/1.3599540
View Table of Contents: http://apl.aip.org/resource/1/APPLAB/v98/i24
Published by the American Institute of Physics.

Epitaxial growth of high mobility Bi_2Se_3 thin films on CdS

X. F. Kou,[1] L. He,[1,a)] F. X. Xiu,[1] M. R. Lang,[1] Z. M. Liao,[2] Y. Wang,[1,2] A. V. Fedorov,[3] X. X. Yu,[1] J. S. Tang,[1] G. Huang,[1] X. W. Jiang,[1] J. F. Zhu,[1] J. Zou,[2] and K. L. Wang[1,a)]
[1]*Department of Electrical Engineering, Device Research Laboratory, University of California, Los Angeles, California 90095, USA*
[2]*Division of Materials and Centre for Microscopy and Microanalysis, The University of Queensland, Brisbane, Queensland 4072, Australia*
[3]*Advanced Light Source Division, Lawrence Berkeley National Laboratory, Berkeley, California 94720, USA*

(Received 18 April 2011; accepted 23 May 2011; published online 13 June 2011)

We report the experiment of high quality epitaxial growth of Bi_2Se_3 thin films on hexagonal CdS (0001) substrates using a solid source molecular-beam epitaxy system. Layer-by-layer growth of single crystal Bi_2Se_3 has been observed from the first quintuple layer. The size of surface triangular terraces has exceeded 1 μm. Angle-resolved photoemission spectroscopy clearly reveals the presence of Dirac-cone-shape surface states. Magneto-transport measurements demonstrate a high Hall mobility of $\sim$6000 cm^2/V s for the as-grown Bi_2Se_3 thin films at temperatures below 30 K. These characteristics of Bi_2Se_3 thin films promise a variety of potential applications in ultrafast, low-power dissipation devices. © *2011 American Institute of Physics*. [doi:10.1063/1.3599540]

Topological insulators (TIs) have become the most intriguing materials in condensed matter physics and material science ever since the prediction of the existence of their non-trivial surface states.[1–3] In 2009, three-dimensional TIs of Bi_2Se_3, Bi_2Te_3, and Sb_2Te_3 were first proposed by Zhang *et al.* and have been globally focused thereafter.[4] Although semiconductor behaviors are maintained in the bulk, the surface states display a Dirac-cone-like dispersion relationship due to strong spin-orbit interaction, and the surface conductance should be protected by the time-reversal-symmetry (TRS).[4–6] The nature of this surface state provides a variety of fascinating physical phenomena, and the gapless surface also enables quasi-superconducting transport.[7–14] All of these unique properties make TIs one of the most promising candidates for nanoelectronics, spintronics, and quantum computing applications.[10,12,15]

Recently, TI thin films grown by MBE have been reported on Si(111),[16–21] SiC (0001),[22] GaAs (111),[23] and other insulating substrates like α-Al_2O_3 (0001)[24] and $SrTiO_3$ (111).[25] However, these substrates so far have relatively large lattice mismatch with the grown TI materials, resulting in a (quasi-) Van der Waals growth at the early stage of growth, so that the sizes of surface terraces were limited within 300 nm. Moreover, the film qualities were further restricted by the sacrificial layers at the interface, such as the Bi wetting layer or amorphous layers which are used to suppress the dangling bonds and decouple the thin films from their underlying substrates.[17,21] Such drawbacks can greatly degrade the transport properties.

In this letter, we report the epitaxial growth of high-quality Bi_2Se_3 films on the lattice-matched insulating substrate material, i.e., hexagonal CdS (0001), using a solid source MBE system. We demonstrate the crystalline of Bi_2Se_3 starting from the first quintuple layer (QL). More importantly, we show a good surface quality of the grown Bi_2Se_3 thin film with the largest triangular terrace sizes grown by MBE that far. This surface improvement also produces a high Hall mobility at low temperatures, and makes the TI based high-speed devices possible.

Experimentally, our MBE growth was performed in an ultrahigh vacuum system. The epi-ready semi-insulating CdS (0001) substrates (E_g=2.42 eV) with a resistivity of 10^7 Ω·cm were first degassed at 400 °C inside the MBE chamber for 2 h before sample growth. The epitaxial growth was conducted under a Se-rich environment, and detail growth information can be found elsewhere.[20]

In-situ growth dynamics were monitored by real-time high-energy electron diffraction (RHEED) measurements. The sharp streaky patterns in Fig. 1(a) indicate the atomically flat surface morphology during the growth. The intensity of the specula spot was tracked, as shown in Fig. 1(b). The layer-by-layer RHEED oscillations were clearly observed right at the beginning of the growth, which provides strong evidence of epitaxial growth from the first layer. Meanwhile, by fitting the oscillation curve with a damped sinusoidal function, the growth rate can be estimated as 0.55 QL/min.

Atomic force microscope (AFM) was performed to investigate the surface morphology of the Bi_2Se_3 thin film. Figure 1(c) shows a typical AFM image of an as-grown Bi_2Se_3 film with a thickness of 49 QLs. Characteristically, triangle-shaped terraces were observed. Compared with reported data, the terrace size of our Bi_2Se_3 thin films was significantly increased to $\sim$1 μm, and the root mean square (RMS) surface roughness was well controlled to below 0.5 nm. This extraordinary improvement of the surface quality comes from the advantage of the epitaxial growth of the lattice-matched Bi_2Se_3–CdS system (note a_{BiSe} =4.13 ± 0.1 Å and a_{CdS}=4.138 Å)[18,26] which inherently promotes a smooth two-dimensional (2D) growth without having sacrificial amorphous layers at the initial growth. Furthermore, Fig. 1(d) shows the height profile of the red solid line marked in Fig. 1(c). The height of each step is $\sim$0.95 nm, which is consistent with the reported thickness of one individual Bi_2Se_3 QL.[27] In order to understand the

a)Author to whom correspondence should be addressed. Electronic mail: liang.heliang@gmail.com.

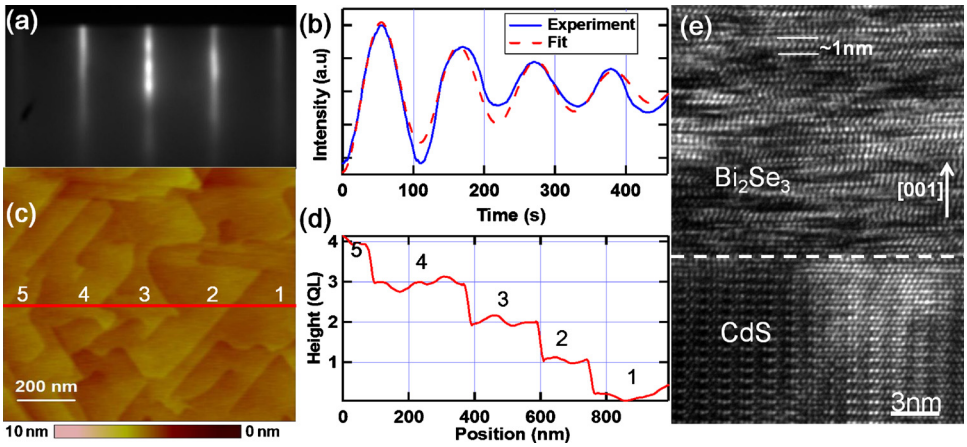

FIG. 1. (Color online) (a) RHEED pattern along [11$\bar{2}$0] direction of an as-grown surface of Bi_2Se_3 with a thickness of 49 QLs. (b) RHEED oscillations of intensity measured (blue, solid) and fitted curve (red, dashed) of the specular beam. The oscillation period is found to be 110 s, corresponding to a growth rate of ~0.55 QL/min. (c) AFM image of the Bi_2Se_3 thin film with the size of 1 μm × 1 μm. (d) The height profile along the solid red line marked in (c), showing a step size of 0.95 nm. (e) HRTEM of a Bi_2Se_3 grown on a CdS (0001) substrate.

interface between the substrate and the Bi_2Se_3 thin film, high-resolution transmission electron microscopy (HRTEM) was performed and the result is shown in Fig. 1(e), in which atomically flat interface is clearly observed, as marked by a dashed line. This result is consistent with our real-time RHEED observation outlined above. The layered structures of the single crystal Bi_2Se_3 are clearly seen in Fig. 1(e) and no amorphous layer or other sacrificial layer in the interface can be observed. The lattice spacing between (0003) planes is measured to be ~1 nm, as indicated by two paralleled white lines in Fig. 1(e), which agrees with other reports.[17,20]

The electronic structure of the Bi_2Se_3 thin film grown on CdS substrate was studied by angle-resolved photoemission spectroscopy (ARPES). Samples with atomically clean surfaces suitable for ARPES were prepared by mild annealing at T=200 °C in the experimental chamber for two hours. All photoemission data were collected from the samples kept at room temperature. Figure 2(a) displays the core level photoemission from Bi_2Se_3 thin film using 100 eV photons. Two spin-orbit split doublets at binding energies of ~54 eV and 24 eV correspond to the 3*d* states of Se and 5d states of Bi atoms respectively. Observation of the unreconstructed and sharp pattern of the low energy electron diffraction (LEED) further confirmed the good surface quality of our epitaxial films of Bi_2Se_3 [inset in Fig. 2(a)].[18] Fig. 2(b) shows ARPES data revealing clearly visible Dirac cone. The Dirac point is located at 350 meV below the Fermi level.

Magnetotransport measurements were performed on standard Hall bars which were fabricated using photolithography process. The typical structure of the devices is sketched in Fig. 3(a) with the device size of 10 μm(*L*) × 40 μm(*W*). Figure 3(b) shows the temperature dependence of the longitudinal resistance R_{xx}. Three distinctive regions can be observed in this plot. The relation from the room temperature first exhibited a metal-like behavior, where the resistance decreased monotonically with the reduced temperature. The freeze-out of the bulk carriers occurred at the region between 40 and 80 K, which caused a rise in resistivity with decreasing the temperature. Finally in the lower temperature regions, the resistivity saturated.

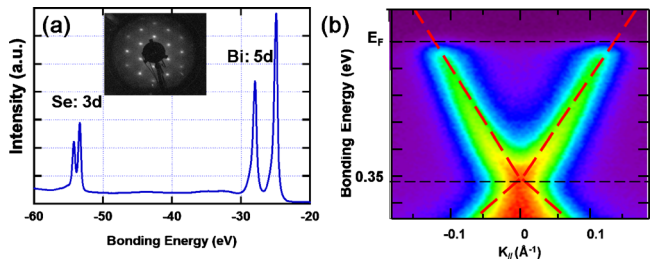

FIG. 2. (Color online) (a) Core level photoemission of the Bi_2Se_3 thin film grown on the CdS substrate with the thickness of 49 QL. Both Se and Bi core levels are measured with 100 eV photons. Inset: LEED pattern of the Bi_2Se_3 thin film showing a (1 × 1) plane structure. (b) ARPES intensity map of the 49 QL Bi_2Se_3 thin film along Γ-K direction. The data were taken using 52 eV photons.

To analyze quantitatively the transport performance, the influences of temperature on the carrier density and mobility were investigated. The unique activation behavior can be clearly observed by plotting the logarithm of carrier density with 1/*T*. In the freeze-out region, it followed perfectly with the Arrhenius relation, and the activation energy was 20 meV, as shown by the solid blue line in Fig. 3(c). This is probably due to a shallow impurity band located 20 meV below the bulk conduction band.[28] Meanwhile, the sheet carrier density approached a constant value of 5.8×10^{13} cm^{-2} below 40 K. This observation is consistent with reported data,[20,29] suggesting that the contribution of bulk carriers has been partially suppressed, and the surface becomes dominant at very low temperatures.

Carrier mobility as a function of temperature is also plotted in Fig. 3(d). In the high temperature region (40–300 K), the power-law function is most likely a consequence of phonon scattering. The scaling factor of our experimental data was fitted to be $T^{-1.7}$. On the other hand, the mobility was saturated and reached above 6000 cm^2/V s when the temperature fell below 30 K. This Hall mobility exceeds previously reported data,[17,22] and is also comparable with those obtained by other chemical methods.[29,30] Such enhanced mobility is attributed from the good surface quality. When the majority of the bulk carriers are frozen out at very low temperature, the surface conductance component begins to become more prominent. For an idea flat 2D surface, backscattering should be prevented owing to the TRS held by TI materials.[10] However, isolated terraces were inevitably formed on the surface during growth. This surface roughness would possibly result in inter-terrace scattering, and thus degrades the mobility. Alternatively, this degradation can be effectively inhibited once the terrace density is reduced. This explains the case of our thin film growth on the CdS substrate as evidenced in Fig. 1. It should be noted that the mobility we obtained is the effective value because the overall conductance is the superposition of both the surface and

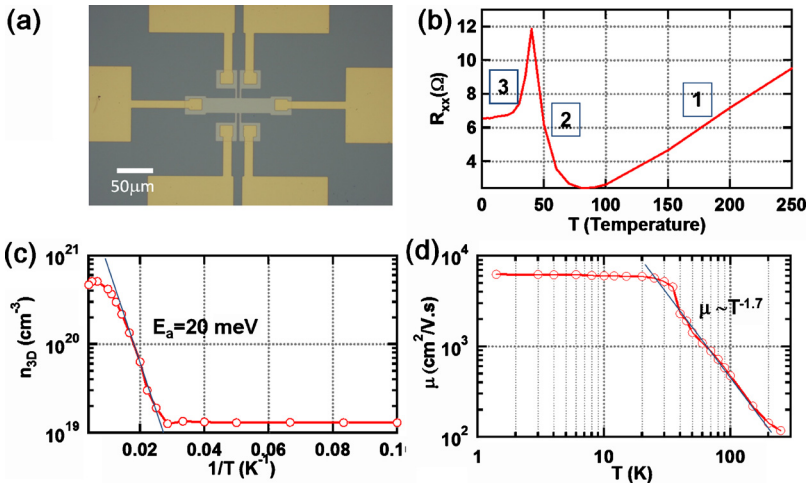

FIG. 3. (Color online) (a) Bi_2Se_3 49 QL Hall bar device structure, with the size of $L \times W = 10\ \mu m \times 40\ \mu m$. (b) The dependence of the device longitudinal resistance R_{xx} on temperature. Three regions are marked, with metal-like behavior in region 1, bulk carrier frozen-out in region 2, and carrier saturation in region 3, respectively. (c) Carrier density of the 49 QL-thick Bi_2Se_3 thin film grown on the CdS substrate as a function of $1/T$. The activation energy in the bulk is 20 meV. (d) Hall mobility vs temperature of the Bi_2Se_3 Hall bar. The mobility scales as $T^{-1.7}$ when $T > 40$ K.

the bulk. Therefore, to extract the accurate value of surface mobility, thickness dependence measurements should be added in future experiments.

In conclusion, we have demonstrated high quality epitaxial growth of Bi_2Se_3 thin films on lattice matched CdS substrate using MBE. The AFM results reveal a good surface morphology and the largest triangular terrace size around 1 μm. HRTEM experiments show no amorphous layer at the interface, on the contrast of the interface on Si (111),[20] indicating that the layer-by-layer growth mode is achieved from the very beginning. The ARPES data demonstrate the single Dirac-cone-like nontrivial surface state with the Fermi level located within the bulk band gap. More importantly, the Hall bar device fabricated on our Bi_2Se_3 thin films exhibits a high Hall mobility of more than 6000 $cm^2/V\,s$ under low temperature. This can be attributed to the suppression of interterrace scattering with improved thin film quality. It is important to further increase the terrace and step sizes so that better transport properties can be achieved on the lattice-matched CdS substrate. This thin film quality improvement will provides an important step toward the realization of innovations for future nanoelectronics and spointronics devices.

This work is supported by the Focus Center Research Program-Center on Functional Engineered Nano Architectonics (FENA) and the Australian Research Council. X. F. Kou and L. He contribute equally to this paper. Y. Wang thanks the Queensland International Fellowship.

[1]L. Fu and C. L. Kane, Phys. Rev. B **76**, 045302 (2007).
[2]L. Fu, C. L. Kane, and E. J. Mele, Phys. Rev. Lett. **98**, 106803 (2007).
[3]J. E. Moore and L. Balents, Phys. Rev. B **75**, 121306(R) (2007).
[4]H. J. Zhang, C. X. Liu, X. L. Qi, X. Dai, Z. Fang, and S. C. Zhang, Nat. Phys. **5**, 438 (2009).
[5]Y. L. Chen, J. G. Analytis, J. H. Chu, Z. K. Liu, S. K. Mo, X. L. Qi, H. J. Zhang, D. H. Lu, X. Dai, Z. Fang, S. C. Zhang, I. R. Fisher, Z. Hussain, and Z. X. Shen, Science **325**, 178 (2009).
[6]Y. Xia, D. Qian, D. Hsieh, L. Wray, A. Pal, H. Lin, A. Bansil, D. Grauer, Y. S. Hor, R. J. Cava, and M. Z. Hasan, Nat. Phys. **5**, 398 (2009).
[7]C. L. Kane and E. J. Mele, Phys. Rev. Lett. **95**, 146802 (2005).
[8]B. A. Bernevig, T. L. Hughes, and S. C. Zhang, Science **314**, 1757 (2006).
[9]M. Konig, S. Wiedmann, C. Brune, A. Roth, H. Buhmann, L. W. Molenkamp, X. L. Qi, and S. C. Zhang, Science **318**, 766 (2007).
[10]X. L. Qi and S. C. Zhang, Phys. Today(1) **63**, 33 (2010).
[11]X. L. Qi, T. L. Hughes, and S. C. Zhang, Phys. Rev. B **78**, 195424 (2008).
[12]J. E. Moore, Nature (London) **464**, 194 (2010).
[13]R. D. Li, J. Wang, X. L. Qi, and S. C. Zhang, Nat. Phys. **6**, 284 (2010).
[14]L. Fu and C. L. Kane, Phys. Rev. Lett. **100**, 096407 (2008).
[15]J. Moore, Nat. Phys. **5**, 378 (2009).
[16]T. Zhang, P. Cheng, X. Chen, J. F. Jia, X. C. Ma, K. He, L. L. Wang, H. J. Zhang, X. Dai, Z. Fang, X. C. Xie, and Q. K. Xue, Phys. Rev. Lett. **103**, 266803 (2009).
[17]H. D. Li, Z. Y. Wang, X. Kan, X. Guo, H. T. He, Z. Wang, J. N. Wang, T. L. Wong, N. Wang, and M. H. Xie, New J. Phys. **12**, 103038 (2010).
[18]G. H. Zhang, H. J. Qin, J. Teng, J. D. Guo, Q. L. Guo, X. Dai, Z. Fang, and K. H. Wu, Appl. Phys. Lett. **95**, 053114 (2009).
[19]Y. Zhang, K. He, C. Z. Chang, C. L. Song, L. L. Wang, X. Chen, J. F. Jia, Z. Fang, X. Dai, W. Y. Shan, S. Q. Shen, Q. Niu, X. L. Qi, S. C. Zhang, X. C. Ma, and Q. K. Xue, Nat. Phys. **6**, 584 (2010).
[20]L. He, F. Xiu, Y. Wang, A. V. Fedorov, G. Huang, X. Kou, M. Lang, W. P. Beyermann, J. Zou, and K. L. Wang, J. Appl. Phys. **109**, 103702 (2011).
[21]Y. Y. Li, G. A. Wang, X. G. Zhu, M. H. Liu, C. Ye, X. Chen, Y. Y. Wang, K. He, L. L. Wang, X. C. Ma, H. J. Zhang, X. Dai, Z. Fang, X. C. Xie, Y. Liu, X. L. Qi, J. F. Jia, S. C. Zhang, and Q. K. Xue, Adv. Mater. (Weinheim, Ger.) **22**, 4002 (2010).
[22]C. L. Song, Y. L. Wang, Y. P. Jiang, Y. Zhang, C. Z. Chang, L. L. Wang, K. He, X. Chen, J. F. Jia, Y. Y. Wang, Z. Fang, X. Dai, X. C. Xie, X. L. Qi, S. C. Zhang, Q. K. Xue, and X. C. Ma, Appl. Phys. Lett. **97**, 143118 (2010).
[23]A. Richardella, D. M. Zhang, J. S. Lee, A. Koser, D. W. Rench, A. L. Yeats, B. B. Buckley, D. D. Awschalom, and N. Samarth, Appl. Phys. Lett. **97**, 262104 (2010).
[24]C. Z. Chang, K. He, M. H. Liu, Z. C. Zhang, X. Chen, L. L. Wang, X. C. Ma, Y. Y. Wang, and Q. K. Xue, arXiv:1012.5716v1 (2010).
[25]J. Chen, H. J. Qin, F. Yang, J. Liu, T. Guan, F. M. Qu, G. H. Zhang, J. R. Shi, X. C. Xie, C. L. Yang, K. H. Wu, Y. Q. Li, and L. Lu, Phys. Rev. Lett. **105**, 176602 (2010).
[26]U. Hotje, C. Rose, and M. Binnewies, Solid State Sci. **5**, 1259 (2003).
[27]H. Lind, S. Lidin, and U. Haussermann, Phys. Rev. B **72**, 184101 (2005).
[28]E. Ohta and M. Sakata, Solid-State Electron. **22**, 677 (1979).
[29]H. Steinberg, D. R. Gardner, Y. S. Lee, and P. Jarillo-Herrero, Nano Lett. **10**, 5032 (2010).
[30]F. Xiu, L. He, Y. Wang, L. Cheng, L.-T. Chang, M. Lang, G. Huang, X. Kou, Y. Zhou, X. Jiang, Z. Chen, J. Zou, A. Shailos, and K. L. Wang, Nat. Nanotechnol. **6**, 216 (2011).